ELSEVIER

Polymer 41 (2000) 2591–2602

polymer

Diffusion and reaction of epoxy and amine in polysulfone studied using Fourier transform infrared spectroscopy: experimental results

G. Rajagopalan[a], K.M. Immordino[a,1], J.W. Gillespie Jr.[a,b,*], S.H. McKnight[c]

[a]Center for Composite Materials and Department of Materials Science and Engineering, University of Delaware, Newark, DE 19716, USA
[b]Department of Civil and Environmental Engineering, University of Delaware, Newark, DE 19716, USA
[c]Army Research Laboratory, Materials Directorate, Aberdeen Proving Grounds, MD, USA

Received 22 February 1999; received in revised form 7 June 1999; accepted 10 June 1999

Abstract

Multi-component diffusion of a diglycidyl ether of bisphenol A (DGEBA) epoxy and an aliphatic diamine, bis(*p*-aminocyclohexyl)-methane (PACM 20) into amorphous polysulfone (PSU) using a Fourier Transform Infrared Spectroscopy-Attenuated Total Reflectance (ATR-FTIR) technique has been studied. Results indicated that the diffusion of the larger epoxy molecule in polysulfone occurred more quickly when diffusing in the presence of the amine. This behavior and slight deviation of the experimental data from classical Fickian kinetics for amine diffusion into polysulfone were attributed to a finite amount of polysulfone swelling. The diffusion of a model end-capped (non-reactive) epoxy into a polysulfone film saturated with amine was studied to quantify the effect of the amine-induced polysulfone swelling on the diffusivity of the second component. In the DGEBA/PACM 20 system, simultaneous diffusion and reaction in PSU was quantified. Reaction rates in the PSU did not significantly deviate from intrinsic reaction rates of the bulk material. SEM studies of etched epoxy–amine–PSU interphases reveal a semi-interpenetrating network of cured epoxy–amine ranging from 0.6 to 2.4 μm, depending on the processing temperature. The formation of this interphase structure is the primary method of load transfer between these dissimilar materials. This work demonstrates the diffusion, subsequent reaction, and final phase separation as the mechanism for interphase formation in the polysulfone/epoxy-amine system studied. © 1999 Elsevier Science Ltd. All rights reserved.

Keywords: Epoxy–amine/polysulfone; Swelling; ATR-FTIR

1. Introduction

Recent studies have shown that adhesion between thermosets and thermoplastics can be dramatically improved when interdiffusion is possible [1–4]. Examination of certain thermoset–thermoplastic interfaces has shown that thermoset monomers will readily diffuse into compatible thermoplastic resins before complete cure. The resulting graded interphase may enhance bond strength through entanglements between the thermoplastic polymer chains and the network structure of the thermoset.

In earlier work, Immordino et al. [3,5] examined the single component diffusion of DGEBA epoxy and PACM 20 amine into amorphous polysulfone at several temperatures. These studies revealed that the lower molecular weight amine will diffuse faster than epoxy at a given temperature (Fig. 1). The epoxy demonstrated Fickian diffusion behavior, while the amine exhibited slight deviations from ideal Fickian behavior, which was attributed to polysulfone swelling. The study also demonstrated that the interphase size could be controlled through processing conditions and ranged from 4 to 12 μm over the temperature range of 60–100°C. Immordino also showed that the fracture toughness of the dissimilar material bonded joints increased with the size of the interphase and could therefore be tailored during processing.

The case of simultaneous epoxy and amine diffusion in PSU complicates the diffusion and reaction analysis. The polysulfone swelling induced by the faster diffusing amine may change the diffusion behavior of the lagging epoxy molecules. This effect must be examined in order to accurately determine and predict the composition of the polysulfone/epoxy–amine interphase. Also, the curing reaction that occurs between the epoxy and amine will have a dramatic effect on the epoxy and amine diffusivity rates, and on the composition and physical properties of the interphase. The

---

* Corresponding author. Center for Composite Materials and Department of Materials Science and Engineering, University of Delaware, Newark, DE 19716, USA. Tel.: +302-831-8702; fax: +302-831-8525.

E-mail address: gillespie@ccum.udel.edu (J.W. Gillespie Jr.)

[1] Present address: GE Plastics, One Plastics Ave, Pittsfield, MA 01201, USA.

0032-3861/00/$ - see front matter © 1999 Elsevier Science Ltd. All rights reserved.
PII: S0032-3861(99)00418-8

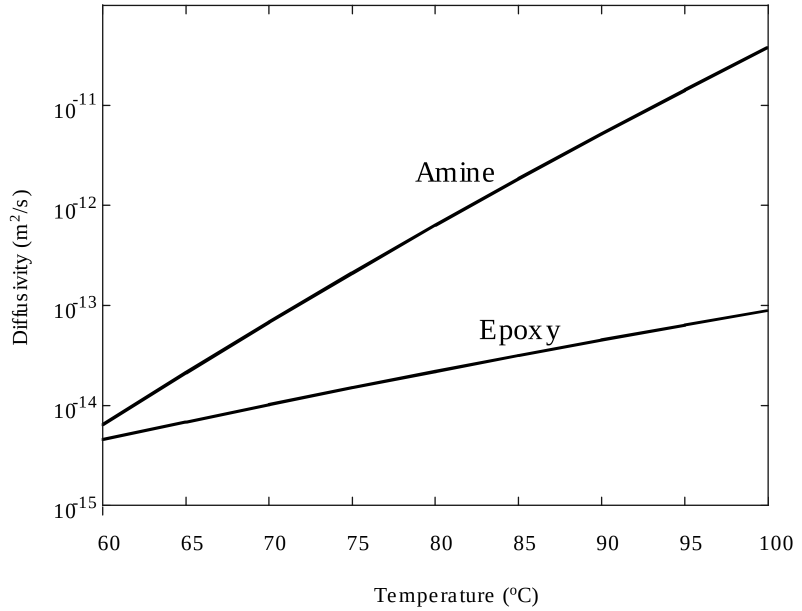

Fig. 1. Epoxy and amine diffusivity vs. temperature [3].

processes of diffusion, swelling, and reaction can be studied using an internal reflection infrared spectroscopic technique (ATR-FTIR) that is able to probe the formation of the polysulfone/epoxy–amine interphase in situ. ATR-FTIR is a powerful spectroscopic technique that has recently been applied to study curing reactions in thermoset polymers at impermeable interfaces [6,7] as well as transport phenomena of small molecules in polymeric systems [8,9]. Recent studies have extended this technique to evaluate polymer–polymer diffusion [3–6,10] and simultaneous diffusion and reaction [3,4].

The present study examines the effects of amine-induced PSU swelling on the diffusion of an end-capped, non-reactive epoxy, and the simultaneous diffusion and reaction processes of an epoxy–amine thermoset system into PSU using the ATR-FTIR technique. The morphology found at the PSU/epoxy–amine interface has been examined using SEM to study the structure of the interpenetrating network formed upon cure.

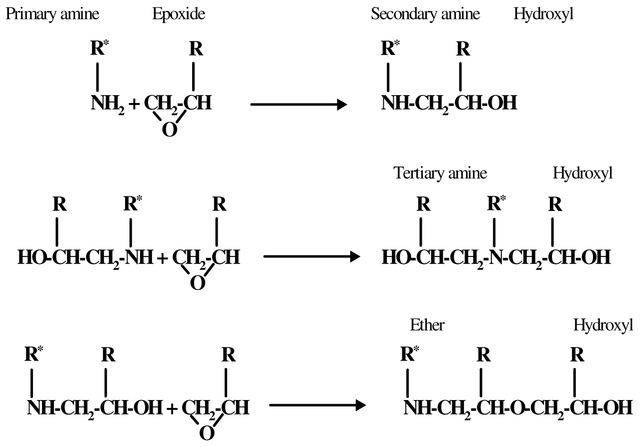

Fig. 2. Schematic of epoxy/amine cure.

2. Experimental

2.1. Materials

Polysulfone (UDEL P1700 from Amoco), an amorphous thermoplastic, was selected for the study to build upon previous findings [1]. A diglycidyl ether of bisphenol A (DGEBA) epoxy resin (Shell, Epon 828) and an aliphatic diamine curing agent, bis-cyclo hexyl diamino methane (PACM 20) were selected for this work. The cure kinetics and properties of the Epon 828/PACM 20 system have been extensively studied [11–13], and a schematic representation of the cure reaction is given in Fig. 2. The diffusivity of the reacting monomers will decrease at or near the gel point, and the diffusion process in the thermoplastic polymer beyond gelation will cease. The time to gelation has been used to predict an upper bound on the diffusion time at any given temperature. Sanford [11] has related the time to gelation using an Arrhenius relationship for the epoxy and amine system studied here:

$$t_{\mathrm{gel}} = 6 \times 10^{-4} \exp\left(\frac{7500}{RT}\right) \mathrm{min} \tag{1}$$

where the activation energy is in cal/mol. Thermodynamically, the enthalpic interactions between pairs of species, which can be described using a Flory–Huggins type of approach, are important. Increasing molecular weights can induce phase separation from a loss of compatibility from changing solubility parameters. Further, the presence of thermoplastic during epoxy–amine cure can alter the

Table 1
Calculated solubility parameters through group contribution methods [16] for the materials used in this study. Subscripts e, a, and tp refer to DGEBA epoxy, PACM amine, and PSU respectively

DGEBA epoxy	Modified epoxy	PACM amine	PSU	$(\delta_e - \delta_{tp})^2$	$(\delta_e - \delta_a)^2$	$(\delta_e - \delta_{tp})^2$
20.0	21.3	18.8	23.7	13.7	1.4	24.01

morphology and the cure kinetics [14,15]. The materials in this work are very compatible based on their calculated solubility parameters, δ, listed in Table 1 [16]. Additionally, the compatibility for binary material combinations in each case was determined by computing the square of the difference between the solubility parameters. This value is proportional to the Flory interaction parameter χ [17–19] given in Eq. (2) for polymer-penetrant systems:

$$\chi = \frac{V_p}{RT}(\delta_{po} - \delta_p)^2 \tag{2}$$

where the subscripts po and p refer to the polymer and penetrant respectively, and V_p is the molar volume of the penetrant. This theory predicts that the best penetrant for a given polymer is one whose solubility parameter is equal or close to that of the polymer, i.e. when χ is small or equal to zero. In this study, it is seen from Table 1 that the epoxy–amine pair is the most compatible, while the amine–PSU pair is the least compatible. Previous studies by Immordino [3] have shown that all three materials are compatible.

A non-reactive, end-capped epoxy was synthesized to isolate the effects of swelling on diffusion of the epoxy into an amine-saturated PSU film. The epoxy prepolymers were end-capped using a nucleophilic reagent to produce alcohol end groups, which are unreactive with the amine. The reaction scheme is outlined in Fig. 5. Sodium methoxide was used to modify the functionality from a reactive epoxy to a non-reactive, end-capped DGEBA-like molecule with hydroxyl functionality. Conversion of the epoxide groups was monitored using transmission FTIR to track the concentration of the epoxide to complete conversion to the end-capped product (see Fig. 6). The solubility parameter, δ, for the reaction product is given in Table 1 and is compared with those for the reactive epoxy, amine, and polysulfone. The change in this parameter indicates that the reaction product can be expected to have comparable solution and diffusion properties to those of the original, reactive monomer.

2.2. Procedure

Single-component swelling studies are conducted by studying the diffusion of modified, end-capped epoxy into amine-saturated PSU (61% volume fraction amine). Two-component diffusion and reaction studies are conducted by studying the diffusion of a 75:25 vol.% epoxy–amine mixture into PSU. A schematic of the experimental set-up is shown in Fig. 3. All experiments were done with germanium crystals. Single-component diffusion studies used crystals coated with 3 μm thick PSU-61% PACM 20 amine film, and two-component diffusion and reaction studies used crystals coated with 100% PSU. Two different thicknesses were used, the larger corresponding to the measured interphase size in this material system [2]. The coated crystal was placed in the cell adjacent to the fluid reservoir and heated to the desired temperature (80°C for single-component diffusion, and 60, 80, and 90°C for two-component diffusion). The resin was introduced once the sample assembly equilibrated at the desired temperature. Spectra were acquired periodically once the reservoir had filled.

2.3. Peak selection, identification and monitoring

In order to use the ATR-FTIR technique to study diffusion, detectable and distinguishable peaks in the spectra of each of the components must be selected. Fig. 4 gives the spectra for the pure components, with the bands tracked, which are also listed in Table 2. Proper selection of bands arising from molecular structure components on each monomer enabled simultaneous measurement of diffusion and reaction. The details for the data reduction are described in Appendix A.

2.4. Morphology studies

Samples of epoxy–amine–PSU were prepared by placing uncured stoichiometric epoxy–amine mixtures in contact

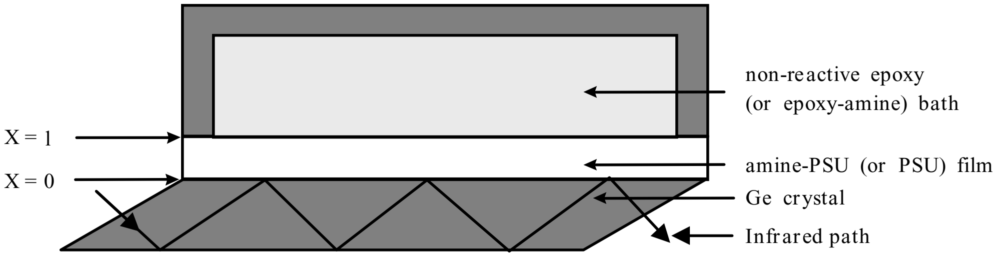

Fig. 3. Sample set-up for swelling and diffusion-reaction studies.

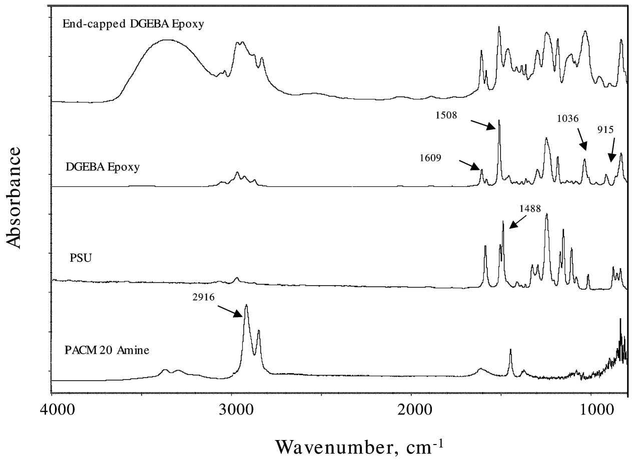

Fig. 4. Spectra of the components used showing bands monitored.

with amorphous PSU at 60, 80, and 90°C for 2 h followed by a post-cure at 160°C for 2 h. After curing, the PSU-rich regions were etched away using methylene chloride leaving the crosslinked epoxy–amine phase behind. The etched surface was viewed from perpendicular and parallel perspectives on a JEOL JXA-840 Scanning Electron Microscope (SEM) after sputter coating with gold. The parallel mode of examination facilitates a study of the sample edge and can help determine the depth of the diffuse interphase.

3. Results and discussion

In this section, results for the single-component and simultaneous diffusion and reaction studies are presented. The Arrhenius relations [5] for the single-component diffusion of epoxy and amine monomers into amorphous PSU are presented, along with the equilibrium concentrations of the amine in PSU in the range studied. The results of the single-component diffusion of end-capped epoxy into amine-saturated PSU are presented to determine the effects of PSU swelling on epoxy diffusivity. The results of the simultaneous diffusion with reaction of epoxy–amine in PSU are presented, and diffusion cessation times for the temperatures studied are determined.

3.1. Single-component diffusion into amorphous PSU

By assuming Fickian diffusion kinetics, Immordino [5] used the ATR-FTIR technique to study the individual diffusion of epoxy and amine monomers into PSU and derived the respective Arrhenius relations. The Arrhenius diffusivity relationship for the epoxy (D_e) and amine (D_a) are:

$$D_e(T) = 52.3 \times 10^{-4} \exp\left(-\frac{18\,500}{RT}\right) \quad (3)$$

$$D_a(T) = 1.044 \times 10^{21} \exp\left(-\frac{54\,000}{RT}\right) \quad (4)$$

where the subscripts e and a refer to the epoxy and amine, respectively, D_e, D_a are in m^2/s, R is the ideal gas constant in cal/(mol K), and T is in Kelvin.

Immordino also determined the equilibrium amine concentrations in PSU in the 50–80°C range. These results are given in Table 3. In the range studied, the equilibrium amine concentration increases from 16 to 58%.

3.2. Single-component diffusion into amine-saturated PSU

Based on Immordino's findings, the swelling study was conducted at 80°C. At this temperature the amine molecules have a significantly higher diffusivity than the epoxy (Fig. 1—the ratio of amine to epoxy Arrhenius diffusivity is 30 [5], while at 60°C it is 1.5). At 80°C, swelling through polymer chain relaxation will occur much more rapidly. Further, the equilibrium amine concentration in the ternary system is also expected to be higher (Table 3) and may result in a further increase in swelling. Hence, based on these considerations a temperature of 80°C was chosen to maximize the sensitivity of the ATR technique to the swelling mechanism.

The normalized absorbance data as a function of time for the 1609 and 1508 cm^{-1} bands from the non-reactive peak are shown in Fig. 7(a), along with the fit of Eq. (A3) to determine the diffusivity D (see Appendix A for details). The absorbance data for the diffusion of the end-capped epoxy into amine-saturated PSU clearly saturates earlier than those for the diffusion of end-capped epoxy into amorphous PSU. This provides convincing evidence that the amine swells the PSU, thereby increasing the epoxy

Table 2
Characteristics of epoxy, amine, and PSU bands monitored

Monomer	Band (cm^{-1})	Chemical group	Depth of penetration (μm)	Chemical nature
Epoxy	915	Epoxide ring	0.54	Reactive
	1036	Aromatic deformation	0.48	Non-reactive
	1508	C–C skeletal stretching	0.33	Non-reactive
	1609	C–C skeletal stretching	0.31	Non-reactive
Amine	2916	Asymmetric cyclohexane ring stretch		
Polysulfone	1488	Aromatic skeletal stretching	0.34	Non-reactive

Table 3
Equilibrium amine concentration in PSU with temperature [3]

Temperature (°C)	Amine (%)
50	16
60	44
80	58

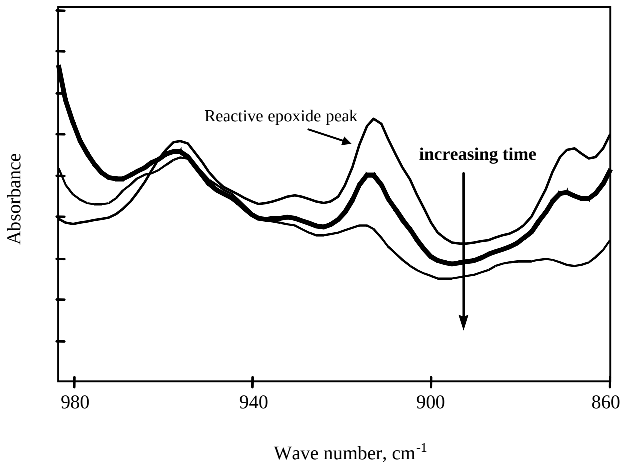

Fig. 6. Decrease of the 915 cm^{-1} epoxide peak with time when reacted with sodium methoxide in methanol.

diffusivity. The effect of the presence of the amine can be quantified by examining the results of the model curve fits. From the results in Table 4, the end-capped epoxy diffusivity into a 61% by volume amine–PSU film appears to be about three times as large as the baseline diffusivity into amorphous PSU. Table 4 also indicates the diffusivity values calculated for the end-capped epoxy and amine peaks monitored. The slight difference in calculated diffusivity values for the two epoxy peaks monitored possibly arises from a difference in the penetration depths at these two wavelengths, as the penetration depth is an indication of the sampling volumes.

Fig. 7(b) shows the decrease of the absorbance data for the 2916 cm^{-1} amine peak during the diffusion of the end-capped epoxy into amine-saturated PSU at 80°C, along with fit of Eq. (A3). This decrease can arise from one of two causes. Assuming that the amine does not diffuse out from the film, a dilution effect can be a cause, as overall volume increases through end-capped epoxy diffusion only into the amine–PSU film. Alternatively, the amine could diffuse from the PSU film to the bath in a direction opposite to that of the end-capped epoxy. However, for a dilution effect, mass conservation necessitates that the apparent diffusivities of the amine and PSU peak absorbances equal the end-capped epoxy diffusivity into the film. Since the calculated diffusivities of the amine and end-capped epoxy are not equal (Table 4), and the PSU concentration does not change appreciably (Table 5), a dilution effect can be eliminated. Hence, the amine diffuses out from the film to the epoxy bath with continuing diffusion of epoxy into the amine-saturated PSU film. This implies that the equilibrium amine concentration in the ternary epoxy–amine–PSU system will be lower than in the binary amine–PSU system at this temperature. Consequently the amount of swelling will be proportionately smaller during the simultaneous diffusion of epoxy and amine into PSU.

The experimental data of the diffusion of the non-reactive epoxy into the amine–PSU film can also be used to estimate the equilibrium concentrations in the ternary system and, specifically, in the interphase. Assuming constant concentration profiles, the equilibrium non-dimensional concentrations of the amine and PSU are determined using the following expressions:

$$c_{\mathrm{a}} = \frac{A_{\mathrm{final}}^{\mathrm{amine}}}{A_{\mathrm{initial}}^{\mathrm{amine}}} \tag{5}$$

$$c_{\mathrm{PSU}} = \frac{A_{\mathrm{final}}^{\mathrm{PSU}}}{A_{\mathrm{initial}}^{\mathrm{PSU}}} \tag{6}$$

where the absorbances corresponding to a characteristic amine and PSU peak are used, respectively. For the epoxy, the following expression is used:

$$c_{\mathrm{e}} = 1 - c_{\mathrm{a}} - c_{\mathrm{PSU}} \tag{7}$$

The results are given in Table 5 along with the initial amine and PSU concentrations in the amine-saturated PSU film. From these results it is evident that amine diffuses out of the amine–PSU film into the non-reactive epoxy bath. Knowledge of the equilibrium concentrations in the ternary epoxy–amine–PSU system is necessary, as it provides an insight into the expected properties and structure of the interphase region. In the present study, it appears that the ratio of the equilibrium epoxy and amine concentrations in PSU is similar to the stoichiometric ratio for optimum properties [20].

The increased epoxy diffusivity from swelling has profound implications for the simultaneous diffusion and reaction of epoxy–amine in PSU and the resulting interphase. A larger interphase is expected due to the enhanced

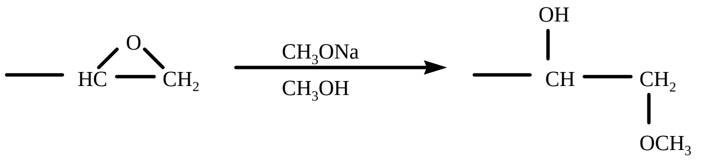

Fig. 5. Ring opening mechanism and nucleophilic attack of the epoxide ring using sodium methoxide.

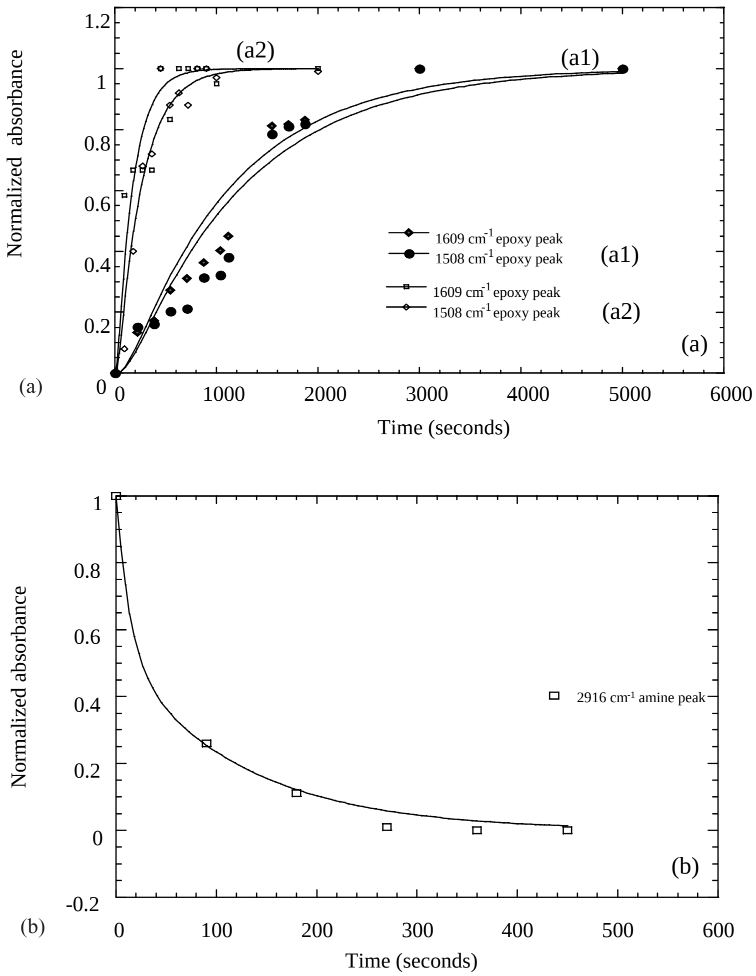

Fig. 7. Single-component diffusion of end-capped epoxy into amine-saturated PSU at 80°C. (a) Baseline end-capped epoxy diffusion into PSU (a1) and end-capped epoxy diffusion into amine-saturated PSU, confirming swelling (a2); (b) 2916 cm^{-1} amine peak absorbance, showing amine diffusion from the amine-saturated PSU film to bath.

diffusivity of the epoxy. Also the relative concentrations of epoxy and amine in the film may more closely match the stoichiometric mixture. It has been reported that epoxies cured with off-stoichiometric amounts of amine have a lower glass transition temperature and compromised mechanical properties [20].

The experiments in this section confirmed that the small amine molecules swell the glassy PSU film. This causes an increase in the diffusivity of the epoxy, which was quantified using the ATR-FTIR experiments. The next section discusses the results of the simultaneous diffusion and reaction of epoxy and amine into PSU, and its implications for interphase formation and size.

3.3. Simultaneous diffusion with reaction of epoxy–amine in PSU

This section discusses the results of the ATR-FTIR study for the non-reactive and reactive epoxy peaks for the

Table 4
Diffusivity of end-capped epoxy into amorphous PSU film and amine–PSU film at 80°C. Numbers in parentheses are the regression coefficients

Peak (cm^{-1})	Epoxy diffusivity into amorphous PSU film, m^2/s	Epoxy diffusivity into amine–PSU film, m^2/s	Amine diffusivity from amine–PSU film, m^2/s
1609	6.5×10^{-15} (0.96)	2.3×10^{-14} (0.90)	–
1508	4.8×10^{-15} (0.99)	1.5×10^{-14} (0.97)	–
2916	–	–	5.7×10^{-14} (0.99)
Average diffusivity	6×10^{-15}	2×10^{-14}	

Table 5
Initial and final (equilibrium) concentrations (% volume fractions) of the non-reactive epoxy, amine, and polysulfone ternary mixture at 80°C

	Non-reactive epoxy	Amine	Polysulfone
$t = 0$	0	61	39
$t = \infty$	51	15	34

DGEBA/PACM 20 system. Further, the effects of reaction on diffusion are also discussed.

3.3.1. Non-reacting epoxy peak

The non-reactive groups (Table 2) are not involved in the epoxy–amine reaction and should change only from reaction effects (i.e. increasing molecular weight) on diffusivity.

Fig. 8 shows the 1036 cm^{-1} DGEBA peak absorbance data measured during the diffusion–reaction experiments using the thin PSU films at 60, 80 and 90°C. Predictions based on the Arrhenius diffusivity expressions in Eqs. (3) and (4) for the individual epoxy and amine monomers are also included in this figure for reference. The effect of PSU swelling is particularly evident at 80°C and 90°C where transient concentrations are much higher than the reference at larger time scales. In the case of 60 and 80°C, the initial uptake of epoxy is slower than at larger times at these temperatures. This sigmoidal behavior is characteristic of swelling where a finite relaxation time exists for the PSU chains to accommodate the penetrant molecules. At 90°C, this behavior is not observed, as the relaxation time must be smaller than the interval chosen to read data.

With the thinner films the absorbances of the epoxy increase rapidly and then drop slightly (at 80 and 90°C) before leveling off (Figs. 9–11). Swelling from the amine increases the PSU volume and is the cause for the noticeable decrease in absorbance for the 1036 cm^{-1} peak.

For the thicker films (6, 10, 12 μm at 60, 80, 90°C, respectively) there was no significant change in absorbance as a function of time. This indicates that the diffusion of epoxy and amine ceased before the monomers reached the penetration depth of the crystal. A reason for this is reaction dominance over diffusion with time at these length scales. This result implies that the interphase size in this material

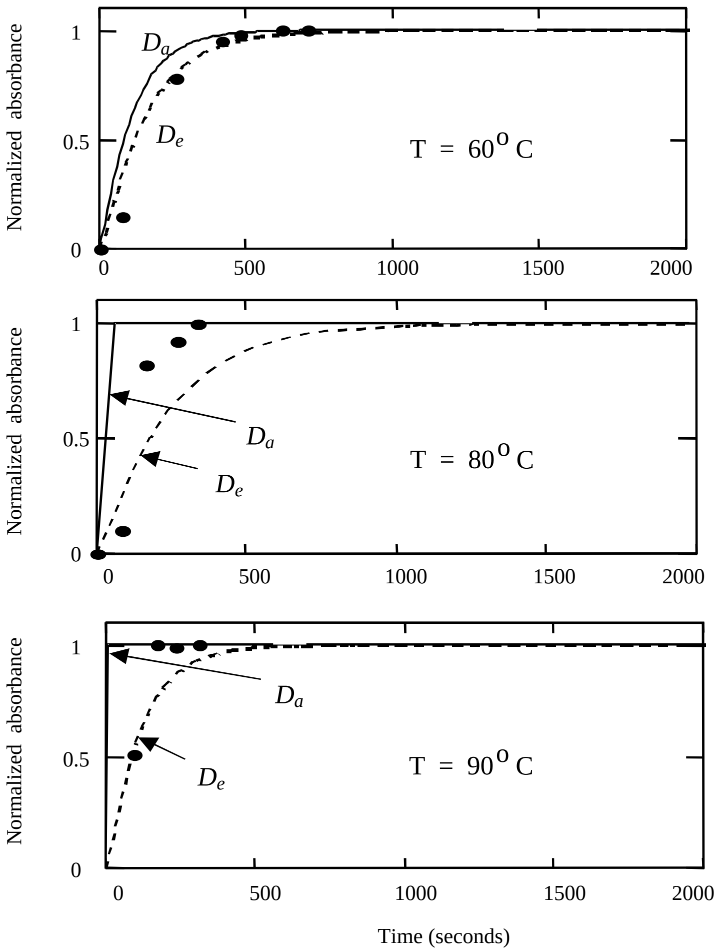

Fig. 8. Comparison of experimental 1036 cm^{-1} peak absorbance with the normalized absorbance predicted using epoxy and amine Arrhenius diffusivities for diffusion only.

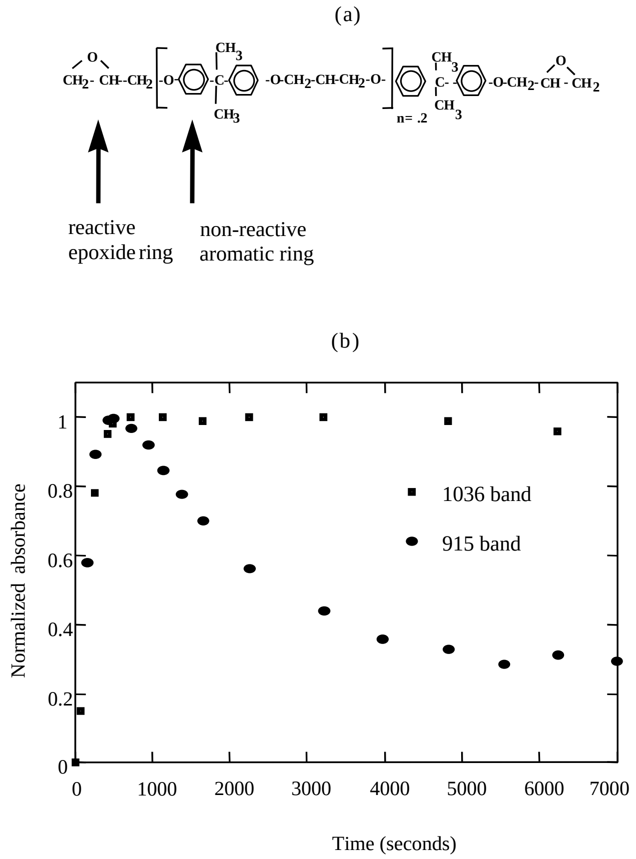

Fig. 9. (a) Structure of the epoxy molecule showing reactive epoxide ring and non-reactive aromatic ring monitored in the ATR-FTIR experiments, and (b) experimental absorbance of reacting (915 cm^{-1}) and non-reacting (1036 cm^{-1}) epoxy peaks in 1.5 μm experiment at 60°C.

system is bound between these film thicknesses at the respective temperatures studied.

3.3.2. Reacting epoxy peak

The 915 cm^{-1} peak corresponds to the epoxide ring on the DGEBA molecule. The normalized absorbance of the 915 cm^{-1} peak during the 1.5 and 4 μm experiments at 60, 80 and 90°C, respectively, can be found in Figs. 9–11. Normalized absorbance is obtained by normalizing over the maximum absorbance difference for the band of interest. Normalized absorbance is plotted along with the non-reacting aromatic 1036 cm^{-1} peak at the same temperature and film thickness for reference. The initial increase due to diffusion followed by the decrease in the absorbance of the 915 cm^{-1} peak is a result of the epoxy–amine curing reaction. The corresponding peak height increase for the OH group deformation at 3400 cm^{-1} agrees with this conclusion. These findings show that the epoxy and amine will cure in the presence of PSU and provide indirect evidence for the formation of an interpenetrating network in the interphase.

Fig. 12 shows the FTIR diffusion data at 80°C plotted on the same time scale as conversion (α) for the epoxy–amine binary system based on the kinetics model of Sanford [11,13] for the system. The FTIR data was fit to an *n*th-order kinetic model for illustrative purposes:

$$\frac{d\alpha}{dt} = K(1-\alpha)^n \tag{8}$$

where K is:

$$K\ (\mathrm{s}^{-1}) = 97\,300\exp\left(-\frac{12\,800}{RT}\right). \tag{9}$$

The fitting parameters are in good agreement with those reported by Sanford [11] and experimental DSC values, indicating that the presence of PSU does not significantly affect the kinetics at low conversions. PSU would be expected to influence cure at higher conversions where diffusion limitations on cure can dominate. A comparison of kinetic parameters, *K*, and reaction orders, *n*, at 80°C can be found in Table 6. The results indicate that the epoxy and amine do react and follow the same kinetic models when in

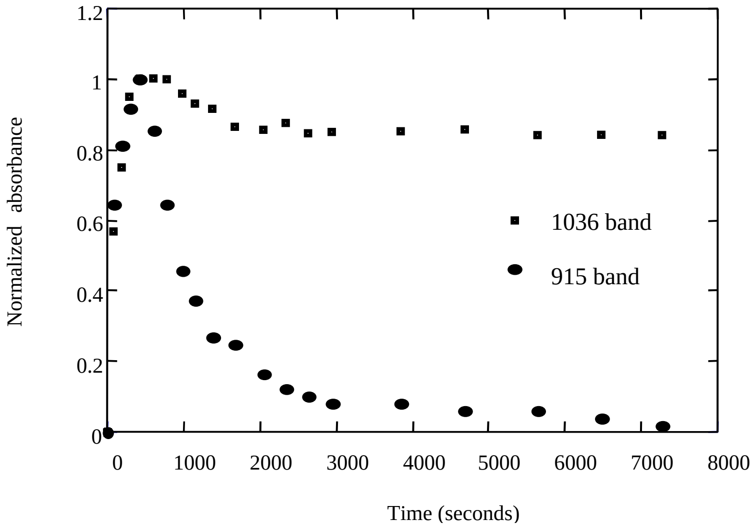

Fig. 10. Experimental absorbance of reacting (915 cm^{-1}) and non-reacting (1036 cm^{-1}) epoxy peaks in 4 μm experiment at 80°C.

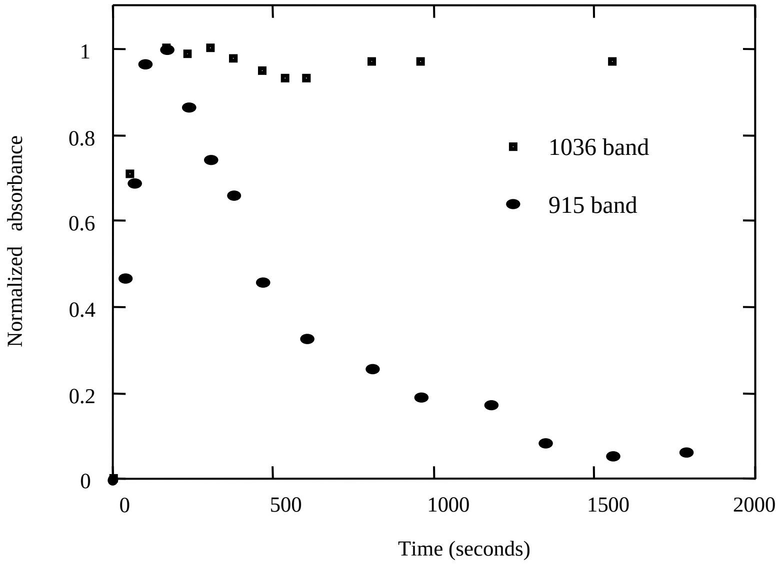

Fig. 11. Experimental absorbance of reacting (915 cm^{-1}) and non-reacting (1036 cm^{-1}) epoxy peaks in 4 μm experiment at 90°C.

the presence of polysulfone at these concentrations. This is a significant result, as the curing causes the formation of an IPN, which contributes to the load transfer between these dissimilar materials.

3.4. Reaction-limited diffusion

This work provides insights into diffusion that becomes limited by the curing reaction. Many researchers have reported that diffusional limitations affect cure at or near the gel point ($\alpha = 0.577$) [21,22]. The diffusion cessation times in the present work can be assumed to occur close to the peak maximum in Figs. 9–11, since monomer diffusion is suppressed beyond this point. Table 7 summarizes the results on predicted times to gelation for a stoichiometric epoxy–amine mixture using Eq. (1) and calculated times to diffusion cessation from the experiments in this study. The corresponding values of the degree of cure, α, are also shown. These values were calculated using the first-order approximation for the DGEBA epoxy–PACM amine cure given in Eq. (8) with $n = 1$ [11].

Sanford's relation for the gel time corresponds to a cure of $\alpha = 0.57$, and it is expected that diffusion ceases prior to this. The experimental results suggest that diffusion essentially ceases much ahead of the gelation times predicted for epoxy-amine cure and is in good agreement with previous findings that suggest that diffusion ceases at a much lower degree of cure [23]. Therefore, the gelation times calculated

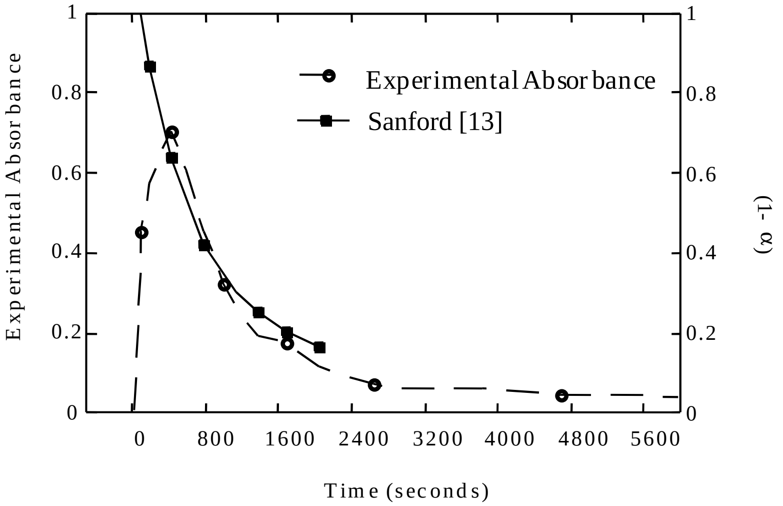

Fig. 12. Comparison of time scales for reaction of epoxy and amine based on *n*th-order kinetics and the decrease in the 915 cm^{-1} peak in epoxy/amine diffusion experiment at 80°C.

Table 6
Comparison of kinetic parameters for epoxy/amine reaction at 80°C

Method	Reaction order, *n*	Constant, *K*
FTIR (915 cm^{-1} peak)	1.34	0.0015
DSC (100:28) no PSU	1.26	0.0013
Sanford (100:28)	1.00	0.0013

from the intrinsic cure kinetics of the thermoset serve as an upper bound for the time scale for interphase formation. Further understanding of these results can be gained by the development of diffusion-reaction models that represent the system accurately [4].

3.5. Morphology studies

The micrographs of the etched epoxy–amine–PSU surface for the samples processed at 60, 80, and 100°C are shown in Figs. 13–15. The figures show the morphology of the ternary blend samples after careful solvent etching of the PSU-rich phase. The etched domains are clearly observed as pits, suggesting that a semi-interpenetrating network was formed in these blends. It is believed that the initially miscible ternary mixture phase separated with continuing epoxy–amine reaction. This reaction leads to increasing molecular weights, resulting in a change of the solubility parameters and loss of miscibility. This observation is consistent with those of Su and Woo [14,15], Woo [24], and others [25,26] who report on the interpenetrating network (IPN) morphology resulting from reaction-induced phase separation in their work with reactive epoxy–amine-thermoplastic systems.

Further the network size decreases with increasing temperature, and this is seen from the finer (smaller) structure at higher temperatures in the micrographs. Table 8 lists the average network, size, with increasing temperature. It is seen that the network size decreases from 2.4 μm at 60°C to 0.6 μm at 100°C. A possible explanation for this trend is that the epoxy–amine reactions proceed to higher conversions at higher temperatures, leading to greater crosslinking and branching [24].

Sample edges were studied to confirm the sizes of these interphases. These studies showed that the length scales of the IPN structures are in close agreement with the interphase sizes given in Ref. [2] in this material system.

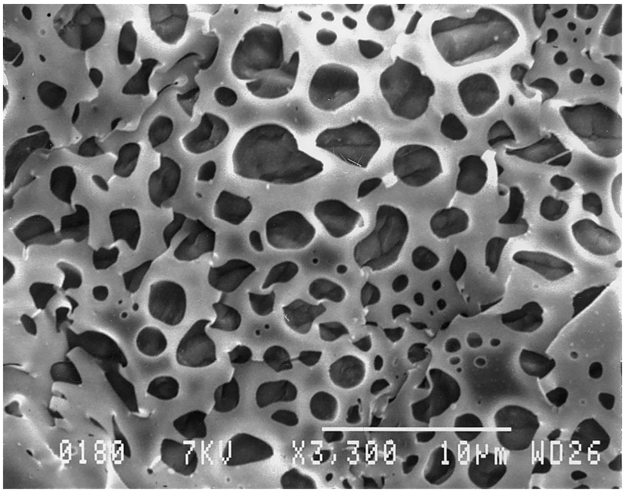

Fig. 13. SEM micrograph of methylene chloride etched DGEBA epoxy–PACM 20/PSU interphase at 60°C showing the formation of an IPN.

4. Conclusions

This study leads to several significant findings. Firstly, experiments with the end-capped epoxy reveal that the small amine molecules swell the glassy polysulfone. Specifically, the amine was shown to swell the PSU network and thereby enhance the epoxy diffusivity by a factor of three. Further, during the two-component reaction–diffusion of epoxy and amine, the epoxy diffusivity increases dramatically from this amine swelling. Additionally, swelling is the most plausible explanation for the slight decrease in absorbance that is observed in the experimental non-reacting epoxy band data at higher temperatures.

Secondly, a mixture of epoxy and amine will diffuse into and react in the presence of PSU. The reaction at 60°C proceeds to partial conversion, characteristic of the intrinsic cure behavior in these thermosets. The structure of the interphase is that of a semi-interpenetrating network of epoxy and amine in PSU, with the network becoming finer at higher temperatures due to a higher degree of crosslink formation through etherification reactions. It is believed that with increasing conversion, phase separation occurs between the curing epoxy–amine and PSU. Hence, the interphase in these material systems arises through three chronological processes: diffusion, reaction, and phase separation.

Experimental results show that the initial time scales for

Table 7
Diffusion times from ATR-FTIR experiments

Temperature (°C)	t_{gel} [11], sec.	α_{gel} [11]	Diffusion time scale (s)	α_{gel} from experiments, using Eq. (8)
60	2272	0.63	479	0.20
80	770	0.63	335	0.35
90	476	0.63	165	0.30

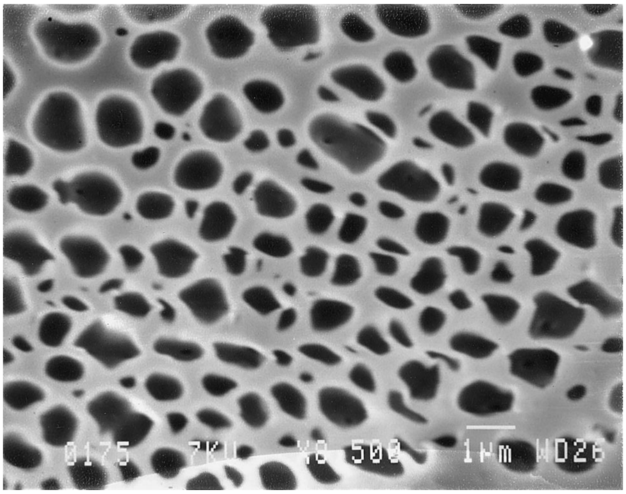

Fig. 14. SEM micrograph of methylene chloride etched DGEBA epoxy–PACM 20/PSU interphase at 80°C.

diffusion are smaller than reaction time scales for all the temperatures studied here. However, diffusivity continuously decreases from increasing epoxy–amine conversion. Hence, after a certain time period (corresponding to the absorbance peak maximum for the 915 cm^{-1} epoxy band) reaction begins to dominate. Hence no further increase in interphase size can be realized beyond this point.

Future work should focus on understanding the effects of reaction on epoxy–amine diffusivity. Development of transport models to better understand the diffusion of reacting thermosets into amorphous thermoplastics is needed. These models should consider the effect of thermoset reaction on the diffusivity, since chain mobility decreases with increasing molecular weight, and concentration in the film, which decreases from reaction after increasing initially from diffusion. Such models can explain better the nature of the absorbance–time curves observed in this work, the difference in ATR-FTIR data for the thinner and thicker film samples, and can be used to determine the interphase size in these material systems as a function of processing conditions.

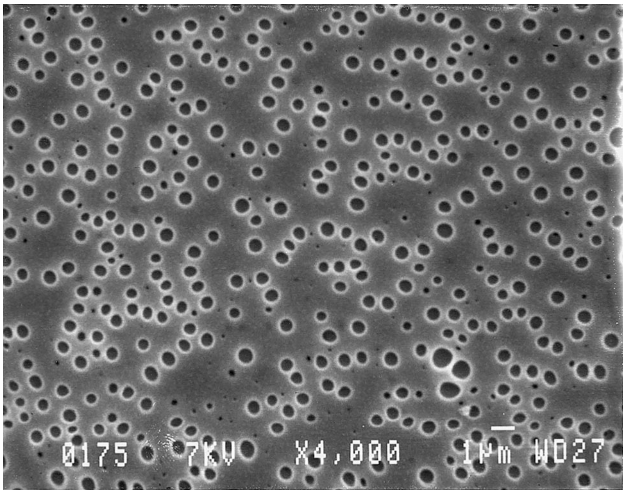

Fig. 15. SEM micrograph of methylene chloride etched DGEBA epoxy–PACM 20/PSU interphase at 100°C.

Table 8
Network size vs. temperature for the epoxy–amine–PSU samples

Temperature (°C)	Size (standard deviation) (μm)
60	2.4 (0.45)
80	0.9 (0.33)
100	0.6 (0.20)

Acknowledgements

This work was supported by the Composite Materials Research Collaborative Program sponsored by the US Army Research Laboratory under Cooperative Agreement DAAL01-96-2-0048.

Appendix A: ATR-FTIR

Diffusion studies using the ATR-FTIR technique have been well described elsewhere [27–29]. In this study germanium internal reflection elements ($n_2 = 4$) with 60° angle of incidence were employed. The values for the depth of penetration in the mid-IR region, therefore, range from 0.16 to 0.54 μm ($n_1 = 1.1$).

In the case of Fickian diffusion through a polymer film on an IRE crystal, the solution to the diffusion equation is as follows [30]:

$$C_\mathrm{p}(x,t) = C_{\mathrm{p},\infty}\left\{1 - \frac{4}{\pi}\sum_{n=0}^{\infty}\frac{(-1)^n}{2n+1}\cos\left(\frac{(2n+1)\pi x}{2l}\right) \times \exp\left[-\left(\frac{(2n+1)\pi}{2l}\right)^2 Dt\right]\right\} \tag{A1}$$

where C_p is the penetrant concentration, l is the film thickness, and D is the penetrant diffusivity. The instantaneous measured ATR absorbance during a diffusion experiment can be expressed [29]:

$$A(t) = A_\infty + \frac{32aSl}{\pi}\left\{\sum_{n=1}^{\infty} F_n \exp\left[-\left(\frac{2n+1)\pi}{2l}\right)^2 Dt\right]\right\} \tag{A2}$$

where

$$F_n = \left[\frac{(-1)^n}{2n+1}\frac{l}{d_\mathrm{p}} + \frac{\pi}{4}\exp\left(-2\frac{l}{d_\mathrm{p}}\right)\right] \times \left\{[(2n+1)\pi]^2 + 16(l/d_\mathrm{p})^2\right\}^{-1}$$

By normalizing the absorbance of the desired band to its initial and final values, the following equation is obtained [5]:

$$\frac{A(t)-A_\infty}{A_0-A_\infty}=\frac{\sum_{n=0}^{\infty}F_n\exp\left[-\left(\frac{(2n+1)\pi}{2l}\right)^2Dt\right]}{\sum_{n=0}^{\infty}F_n}. \tag{A3}$$

This expression has one fitting parameter *viz.* the non-reactive epoxy diffusivity, and the optical constants are conveniently missing from this treatment significantly simplifying the data analysis. This expression is not appropriate for the case of diffusion and reaction but in this work will be used to analyze the diffusion of a non-reactive epoxy through amine-swollen polysulfone. The following assumptions are valid in using Eq. (A3) viz. (a) the penetration depth, d_p, is a constant for the band of interest; (b) the ratio of the film thickness to penetration depth, l/d_p, should always be greater than 5 for the analysis to be valid [6]; and (c) the refractive index of the polymer does not change with concentration or composition [6].

References

[1] McKnight SH, Don RC, Scott M, Braem A, Gillespie JW. Experimental investigation of diffusion enhanced adhesive bonding for thermoplastic composites. Conference Proceedings, Society of Plastics Engineers, Annual Technical Meeting, Boston, 1995.
[2] Rajagopalan G, Immordino KM, McKnight SH, Gillespie Jr JW. Proceedings of the 11th Technical Conference of the American Society for Composites. 1996. p. 539.
[3] Immordino KM. Characterization of the polysulfone/epoxy interphase for bonding thermoplastic composites. MS thesis, University of Delaware, Newark, Delaware, 1996.
[4] Rajagopalan G. Diffusion of reacting thermosets into thermoplastics. PhD dissertation, University of Delaware, Newark, Delaware, 1999.
[5] Immordino Jr. KM, McKnight SH, Gillespie JW. J Adhes 1998;65:115.
[6] Skourlis TP, McCullough RL. J Appl Polym Sci 1994;52:1241.
[7] Brill RP, McCullough RL, Palmese GR. Proceedings of the 11th Technical Conference of the American Society for Composites. 1996. p. 576.
[8] Fieldson GT, Barbari TA. Polymer 1993;34:1146.
[9] McKnight Jr. SH, Gillespie JW. J Appl Polym Sci 1971;64:1997.
[10] Rajagopalan G, McKnight SH, Gillespie Jr JW. Annual Technical Conference–ANTEC, Conference Proceedings of the 54th Annual Technical Conference, Part 1. 1996. p. 1225.
[11] Sanford WM. Cure behavior of thermosetting resin composites, PhD dissertation, University of Delaware, Newark, Delaware, 1987.
[12] Skourlis TP. Structure and properties of the interphase in coated carbon fiber epoxy systems, PhD dissertation, University of Delaware, Newark, Delaware, 1995.
[13] Sanford WM, McCullough RL. J Polym Sci: Polym Phys 1990;28:973.
[14] Su CC, Woo EM. Polymer 1995;36:2883.
[15] Su CC, Kuo JF, Woo EM. J Polym Sci Polym Phys 1995;33:2235.
[16] Hansen CM. J Paint Tech 1967;39:505.
[17] Flory PJ. Principles of polymer chemistry. Ithaca, NY: Cornell University Press, 1953.
[18] Huggins ML. Ann N.Y. Acad Sci 1942;43:1.
[19] Flory PJ. J Chem Phys 1942;10:51.
[20] Palmese GR. Origin and influence of interphase material property gradients in thermosetting composites. PhD dissertation, Department of Chemical Engineering, University of Delaware, Newark, Delaware, 1991.
[21] Barton JM. Polymer 1980;21:603.
[22] Kamal MR, Sourour S. Polym Engng Sci 1973;13:59.
[23] Yu W, von Meerwall ED. Macromolecules 1990;23:882.
[24] Woo EM. J Polym Sci Polym Chem 1996;34:781.
[25] Gomez CM, Bucknall CB. Polymer 1993;34:211.
[26] Pearson RA, Yee AF. Polymer 1993;34:3658.
[27] Garton A. Infrared spectroscopy of polymer blends. New York: Oxford University Press, 1992.
[28] Urban MW. Attenuated total reflectance spectroscopy of polymers: theory and practice. Washington, DC: American Chemical Society, 1996.
[29] Harrick NJ. Internal reflectance spectroscopy. Ossining, NY: Harrick Scientific Corporation, 1987.
[30] Crank J. The mathematics of diffusion. Oxford: Clarendon, 1975.